



1 **Validation and application of optimal ionospheric shell height model**
2 **for single-site TEC estimation**

3 Jiaqi Zhao¹, Chen Zhou¹

4 School of Electronic Information, Wuhan University, Wuhan, 430072, China

5 Corresponding to: chenzhou@whu.edu.cn

6

7 **Abstract**

8 We recently proposed a method to establish optimal ionospheric shell height model
9 based on the international GNSS service (IGS) station data and the differential code
10 bias (DCB) provided by Center for Orbit Determination in Europe (CODE) during the
11 time from 2003 to 2013. This method is very promising for DCB and accurate total
12 electron content (TEC) estimation by comparing to traditional fixed shell height method.
13 However, this method is basically feasible only for IGS stations. In this study, we
14 investigate how to apply the optimal ionospheric shell height derived from IGS station
15 to non-IGS stations or isolated GNSS receivers. The intuitional and practical method to
16 estimate TEC of non-IGS stations is based on optimal ionospheric shell height derived
17 from nearby IGS stations. To validate this method, we selected two dense networks of
18 IGS stations located in US and Europe region. Two optimal ionospheric shell height
19 models are established by two reference stations, namely GOLD and PTBB, which are
20 located at the approximate center of two selected regions. The predicted daily optimal
21 ionospheric shell heights by the two models are applied to other IGS stations around



22 these two reference stations. Daily DCBs are calculated according to these two optimal
23 shell heights and compared to respective DCBs released by CODE. The validation
24 results of this method present that 1) Optimal ionospheric shell height calculated by
25 IGS stations can be applied to its nearby non-IGS stations or isolated GNSS receivers
26 for accurate TEC estimation. 2) As the distance away from the reference IGS station
27 becomes larger, the DCB estimation error becomes larger. The relation between the
28 DCB estimation error and the distance is generally linear.

29

30 **Keyword**

31 Ionospheric shell height, Single layer model (SLM), Differential code bias (DCB), Total
32 electron content (TEC)

33

34 **Introduction**

35 Dual-frequency GPS signals propagation are affected effectively by ionospheric
36 dispersive characteristic. While, by taking advantage of this property, ionospheric TEC
37 along the path of signal can be estimated by using differencing the pseudorange or
38 carrier phase observations from dual-frequency GPS signals. Carrier phase
39 leveling/smoothing of code measurement is widely adopted to improve the precision of
40 absolute TEC observations (Mannucci et al. 1998; Horvath and Crozier 2007). In
41 general, it is considered that the derived TEC in carrier phase leveling/smoothing



42 technique consists of slant TEC (STEC), the combination differential code bias (DCB)
43 of satellite and receiver, multipath effects and noise. The DCB is usually considered as
44 the main error source and could be as large as several TECu (Lanyi and Roth 1988;
45 Warnant 1997).

46 For TEC and DCB estimations, mapping function with single layer model (SLM)
47 assumption have been intensively studied for many years. Sovers and Fanselow (1987)
48 firstly simplified the ionosphere to a spherical shell. They set the bottom and the top
49 side of the ionospheric shell as $h-35$ and $h+75$ km, where h is taken to be 350 km above
50 the surface of the earth and allowed to be adjusted. In this model, the electron density
51 was evenly distributed in the vertical direction. Based on this model, Sardón et al. (1994)
52 introduced the Kalman filter method for real-time ionospheric VTEC estimation.
53 Klobuchar (1987) assumed that STEC equals VTEC multiplied by the approximation
54 of the standard geometric mapping function at the mean vertical height of 350 km along
55 the path of STEC. Lanyi and Roth (1988) further developed this model into a single
56 thin-layer model, and proposed the standard geometric mapping function and the
57 polynomial model. The single thin-layer model assumed that the ionosphere is
58 simplified by a spherical thin shell with infinitesimal thickness. Clynych et al (1989)
59 proposed a mapping function in the form of a polynomial by assuming a homogeneous
60 electron density shell between altitudes of 200 and 600 km. Mannucci et al (1998)
61 presented an elevation scaling mapping function derived from extended slab mode.
62 There are also many modified mapping function according to the standard geometric



63 mapping function. Schaer (1999) proposed the modified standard mapping function
64 using a reduced zenith angle. Rideout and Coster (2006) presented a new mapping
65 function which replaces the influence of the shell height by an adjustment parameter,
66 and set the shell height as 450 km. Smith et al (2008) modified the standard mapping
67 function by using a complex factor. Based on the electron density field derived from
68 the international reference ionosphere (IRI), Zus et al (2017) recently developed an
69 ionospheric mapping function at fixed height of 450 km with dependence on time,
70 location, azimuth angle, elevation angle, and different frequencies.

71 Ionospheric shell height is considered to be the most important parameter for
72 mapping function, and the shell height is typically set to a fixed value between 350 and
73 450 km (Lanyi and Roth 1988; Mannucci et al. 1998). Birch et al. (2002) proposed an
74 inverse method for estimate the shell height by using simultaneous VTEC and STEC
75 observations, and suggested the shell height is preferred to be a value between 600 and
76 1200 km. Nava et al. (2007) presented a shell height estimation method by minimizing
77 the mapping function errors, this method is referred as the “coinciding pierce point”
78 technique. Their results indicated that the suitable shell heights for the mid-latitude is
79 400 km and 500 km during the geomagnetic undisturbed conditions and disturbed
80 conditions, respectively. In the case of the low-latitude, the shell height at about 400
81 km is suitable for both quiet and disturbed geomagnetic conditions. Jiang et al. (2018)
82 applied this technique to estimate the optimal shell height for different latitude bands.
83 In their case, the optimal layer height is about 350 km for the entire globe. Brunini et



84 al. (2011) studied the influence of the shell height by using an empirical model of the
85 ionosphere, and pointed out that a unique shell height for whole region does not exist.
86 Li et al. (2017) applied a new determination method of the shell height based on the
87 combined IGS GIMs and the two methods mentioned above to the Chinese region, and
88 indicated that the optimal shell height in China ranges from 450 to 550 km. Wang et al.
89 (2016) studied the shell height for grid-based algorithm by analyzing goodness of fit
90 for STEC. Lu et al. (2017) applied this method to different VTEC models, and
91 investigated the optimal shell heights at solar maximum and at solar minimum.

92 In the recent study by Zhao and Zhou (2018), a method to establish optimal
93 ionospheric shell height model for single station VTEC estimation has been proposed.
94 This method calculates the optimal ionospheric shell height with regards to minimize
95 $|\Delta\text{DCB}|$ by comparing to the DCB released by CODE. Five optimal ionospheric shell
96 height models were established by the proposed method based on the data of five IGS
97 stations at different latitudes and the corresponding DCBs provided by CODE during
98 the time 2003 to 2013. For the five selected IGS stations, the results have shown that
99 the optimal ionospheric shell height models improve the accuracies of DCB and TEC
100 estimation comparing to fixed ionospheric shell height of 400 km in a statistical sense.
101 We also found that the optimal ionospheric shell height show 11-year and 1-year
102 periods and is related to the solar activity, which indicated the connection of the optimal
103 shell height with ionospheric physics.

104 While the proposed optimal ionospheric shell height model is promising for DCB



105 and TEC estimation, this method cannot be implemented to isolated GNSS receivers
106 not belonging to IGS stations. The purpose of this study is to investigate the application
107 of the optimal ionospheric shell height derived from IGS station to non-IGS stations.
108 By considering the spatial correlation of ionospheric electron density, it is intuitional
109 and practical to adopt the optimal ionospheric shell height of a nearby IGS station for
110 the non-IGS stations.

111 The purpose of this study is to investigate the feasibility of applying the optimal
112 ionospheric shell height derived from IGS station to nearby non-IGS GNSS receivers
113 for accurate TEC/DCB estimation. By selecting two different regions in U.S. and
114 Europe with dense IGS stations, we calculate the daily DCBs of 2014 by using the
115 optimal ionospheric shell heights derived from 2003-2013 data of two central stations
116 in two regions. We also try to find the DCB estimation error and its relation to distance
117 away from the central reference station.

118

119 **Method**

120 In (Zhao and Zhou, 2018), we proposed a concept of optimal ionospheric shell height
121 for accurate TEC and DCB estimation. Based on daily data of single site, this approach
122 searches daily optimal ionospheric shell height, which minimizes the difference
123 between the DCBs calculated by VTEC model for single site and reference values of
124 DCB. For a single site, its long-term daily optimal ionospheric shell heights can be
125 estimated and then modeled. In our case, the polynomial model (Lanyi and Roth 1988;



126 Wild 1994) is applied to estimate satellite and receiver DCBs, and the DCBs provided
127 by CODE are used as the reference.

128 In the polynomial model, the VTEC is considered as a Taylor series expansion in
129 latitude and solar hour angle, which is expressed as follows:

$$130 \quad T_v(\varphi, S) = \sum_{i=0}^m \sum_{j=0}^n E_{ij} (\varphi - \varphi_0)^i (S - S_0)^j \quad (1)$$

131 where T_v denotes VTEC. φ and S denote the geographic latitude and the solar
132 hour angle of IPP, respectively; φ_0 and S_0 denote φ and S at regional center.
133 E_{ij} is the model coefficient. m and n denote the orders of the model. A polynomial
134 model fits the VTEC over a period of time. In our case, 8 VTEC models are applied per
135 day, and DCB is considered as constant in one day. Since our analysis is based on long-
136 term single site data, we set m and n to 4 and 3, respectively. Huang and Yuan (2014)
137 applied the polynomial model with the same orders to TEC estimation.

138 Based on the thin shell approximation, the observation equation can be written as:

$$139 \quad T_{os}^{PRN}(\varphi, S) = T_v(\varphi, S) \cdot f(z) + DCB^{PRN} \quad (2)$$

140 where T_{os}^{PRN} is slant TEC calculated by carrier phase smoothing, the superscript PRN
141 denotes GPS satellite. DCB^{PRN} denotes the combination of GPS satellite and receiver
142 DCB. z denotes the zenith angle of IPP. According to Lanyi and Roth (1988), the
143 standard geometric mapping function $f(z)$ is expressed as follows:

$$144 \quad f(z) = 1/\cos(z) \quad (3)$$

$$145 \quad z = \arcsin \frac{Re \cdot \cos El}{Re + h} \quad (4)$$



146 where R_e denotes the earth's radius, El denotes the elevation angle, and h denotes
 147 the thin ionospheric shell height. Note that h also affects the location of IPP.

148 To estimate DCBs, The method above requires a definite thin shell height value.
 149 Conversely, if we get the daily solutions of DCBs, the optimal ionospheric shell height
 150 can be estimated. The optimal ionospheric shell height is assumed to be between 100
 151 and 1000 km and is defined as the shell height with the minimum difference between
 152 DCB^{PRN} and the reference values. This optimization problem can be written as:

$$153 \quad \min_{100 < h < 1000} \text{mean}(|\mathbf{DCB}_{\text{ref}} - \mathbf{DCB}|) \text{ s.t. } \mathbf{T} = \mathbf{\Phi} \cdot \mathbf{E} + \mathbf{\theta} \cdot \mathbf{DCB} \quad (5)$$

154 where h is the daily optimal ionospheric shell height, $\mathbf{DCB}_{\text{ref}}$ denotes the vector of
 155 the reference values of DCBs, s.t. is the abbreviation for subject to,
 156 $\mathbf{T} = \mathbf{\Phi} \cdot \mathbf{E} + \mathbf{\theta} \cdot \mathbf{DCB}$ is the matrix form of all the observation equations in one day, \mathbf{T}
 157 denotes the vector of T_{os} , \mathbf{E} corresponds to the coefficients of the models, \mathbf{DCB} is
 158 the vector of DCB^{PRN} , $\mathbf{\Phi}$ and $\mathbf{\theta}$ are the coefficient matrix of \mathbf{E} and \mathbf{DCB} ,
 159 respectively.

160 After the method above is applied to 11-year data, the estimated optimal
 161 ionospheric shell heights can be modeled by a Fourier series, which is expressed as
 162 follows:

$$163 \quad h(x) = a_0 + \sum_{n=1}^k \left(a_n \cos \frac{2n\pi x}{L} + b_n \sin \frac{2n\pi x}{L} \right) \quad (6)$$

164 where k is the order of Fourier series and is set to 40, a_n and b_n are the model
 165 coefficients, x is the time, and L is the time span which equals to 4018 days. The



166 maximum frequency of model is $40/L \approx 0.01$ per day. By least square method, the model
167 coefficients can be estimated. The estimated daily optimal ionospheric shell height
168 $h(x)$ by the model is then applied to other neighboring stations in this region. By using
169 $h(x)$, we can validate the TEC and DCB estimation.

170

171 **Experiment and Results**

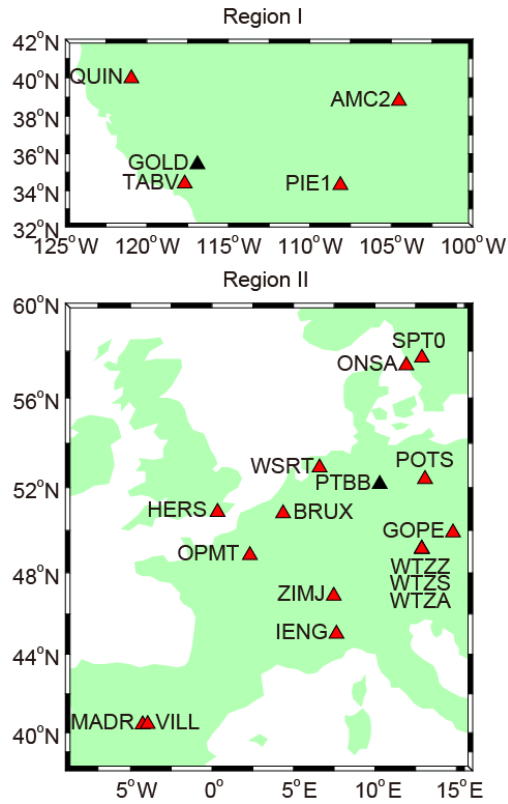
172 The previous section introduced a method to establish daily optimal ionospheric shell
173 height model based on single site with reference values of DCBs. To analyze the
174 improvement of DCB estimation by this model for the reference station and other
175 neighboring stations, we present two experiments to evaluate and validate this method
176 by using IGS stations located in U.S. and Europe region. To ensure the accuracy and
177 consistency of DCB, we only select IGS stations with pseudorange measurements of
178 P1 code, and whose receiver DCBs have been published by CODE.

179 Figure 1 presents the location and distribution of the selected IGS stations in two
180 regions. Table 1 presents the information of the geographical location, distance to
181 reference station in each region and receiver types of all stations. Based on the RINEX
182 data of GOLD station in Region I and PTBB station in Region II during the period of
183 2003-2013, two separate optimal ionospheric shell height models for each region are
184 established by the aforementioned method. Then the model are applied to DCB
185 estimation in 2014 for all the other stations in each region. Note that reference GOLD



186 and PTBB stations are marked with black triangle in the figure. The other neighboring
187 stations are located in different orientations of GOLD and PTBB with different
188 distances, which range from 136 to 1159 km for region I and range from 190.82 to
189 1712.27 km for region II. In the table, the receiver type is corresponding to 2003~2014
190 for GOLD and PTBB, and 2014 for the other stations. In region I, the receiver type of
191 GOLD have been changed once in September 2011. The five selected stations used four
192 receiver types in 2014; TABV and PIE1 had the same receiver type. In region II, there
193 are nine receiver types for the sixteen stations. The receiver type of PTBB have changed
194 twice in 2006.

195



196

197 **Fig.1** Geographical location of the selected IGS stations in U.S. region (Region I) and

198 Europe region (Region II).

199

200

201 **Table 1** Information for the stations

Name	Latitude (deg)	Longitude (deg)	Distance to GOLD or PTBB (km)	Receiver type
GOLD	35.42	-116.89	0	ASHTECH Z-XII3 ~ 2011-09-14 JPS EGGDT 2011-09-19 ~
TABV	34.38	-117.68	136.67	JAVAD TRE_G3TH DELTA
QUIN	39.97	-120.94	619.55	ASHTECH UZ-12



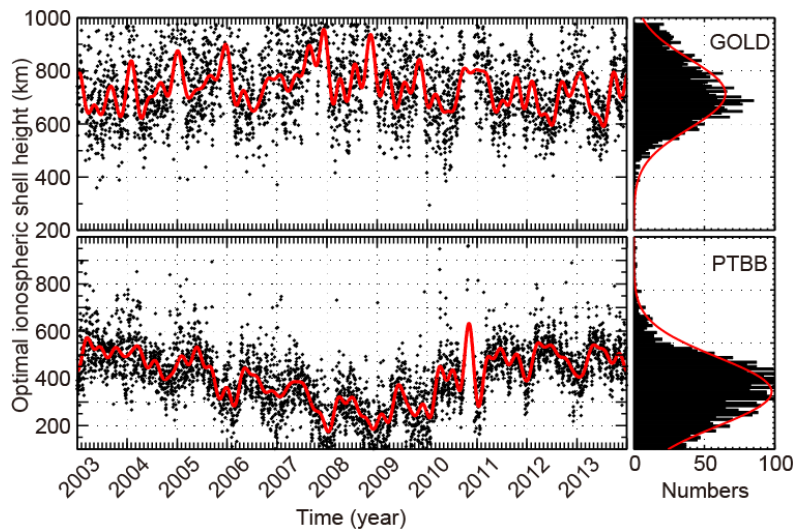
PIE1	34.30	-108.12	810.51	JAVAD TRE_G3TH DELTA
AMC2	38.80	-104.52	1159.09	ASHTECH Z-XII3T
				SEPT POLARX2 2006-07-25~
PTBB	52.15	10.30	0	2006-11-13
				ASHTECH Z-XII3T else
POTS	52.38	13.07	190.82	JAVAD TRE_G3TH DELTA
WSRT	52.91	6.60	264.92	AOA SNR-12 ACT
WTZA	49.14	12.88	381.28	ASHTECH Z-XII3T
WTZS	49.14	12.88	381.28	SEPT POLARX2
WTZZ	49.14	12.88	381.28	JAVAD TRE_G3TH DELTA
GOPE	49.91	14.79	401.51	TPS NETG3
BRUX	50.80	4.36	439.03	SEPT POLARX4TR
ONSA	57.40	11.93	593.72	JPS E_GGD
ZIMJ	46.88	7.47	620.79	JAVAD TRE_G3TH DELTA
SPT0	57.72	12.89	641.78	JAVAD TRE_G3TH DELTA
OPMT	48.84	2.33	674.24	ASHTECH Z-XII3T
HERS	50.87	0.34	705.38	SEPT POLARX3ETR
IENG	45.02	7.64	816.64	ASHTECH Z-XII3T
VILL	40.44	-3.95	1696.62	SEPT POLARX4
MADR	40.43	-4.25	1712.27	JAVAD TRE_G3TH DELTA

202

203 Figure 2 presents the estimated daily optimal ionospheric shell height of GOLD
 204 and PTBB during the period from 2003 to 2013. The left panel shows the variation of
 205 the daily optimal ionospheric shell height and the fitting result by (6). From the overall
 206 trend, the variations of daily optimal ionospheric shell height for both two stations
 207 appear wave-like oscillation during the 11 years period. In the right panel, the statistical



208 result are fitted by a normal distribution. The mean and the standard deviation (STD)
209 of the normal distribution are 714.3 and 185.4 km for GOLD, respectively. The mean
210 and STD value for PTBB is 416.4 and 184.1 km, respectively.
211

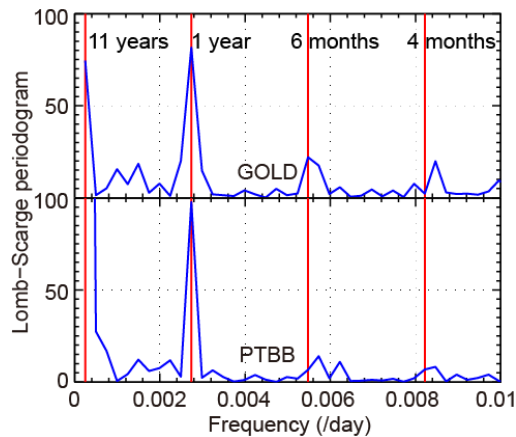


212
213 **Fig.2** Variation of the daily optimal ionospheric shell height (black) and the fitting
214 result (red)

215
216 Figure 3 presents the amplitude spectra of the daily optimal ionospheric shell
217 height of two reference stations estimated by the Lomb-Scargle analysis (Lomb 1976;
218 Scargle 1982). As can be found in Figure 3, the peaks correspond to 11-year, 1-year, 6-
219 month and 4-month cycles. The amplitudes of 11-year and 1-year cycles are more
220 evident than other periods in both two stations. Note that the frequencies above 0.01
221 per day are discarded because of their small amplitudes. As mentioned earlier, 0.01 per
222 day is about the maximum frequency of (6). This result shows that the optimal



223 ionospheric shell height of GOLD and PTBB is periodic, and the 40th-order of Fourier
224 series is suitable for modelling its variation.



225

226 **Fig.3** Lomb-Scargle spectra of the daily optimal ionospheric shell height

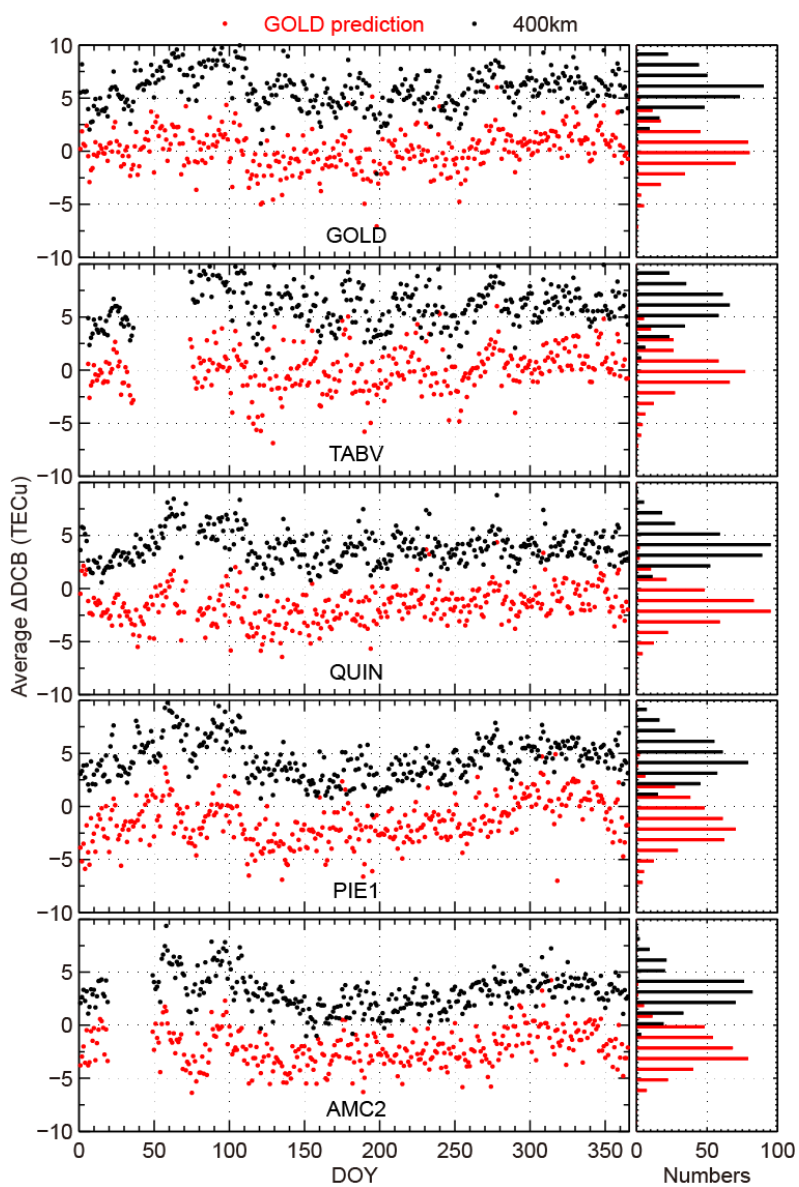
227

228 We establish two optimal ionospheric shell height models for each region by the
229 40th-order of Fourier series based on the 11-year data of GOLD and PTBB. To
230 investigate the availability zone of the optimal ionospheric shell height model, we apply
231 the model to the stations of each region as shown in Figure 1 and Table 1. Based on the
232 predicted daily optimal ionospheric shell heights in 2014 calculated by the model of
233 GOLD and PTBB, the DCBs in all stations of each region are estimated in the form of
234 single station by the polynomial model mentioned earlier. The difference of DCBs in
235 all station in each region calculated by the optimal ionospheric shell height model from
236 each reference station and DCBs provided by CODE is then compared to the difference
237 of DCBs calculated by fixed ionospheric shell height (400 km) and DCBs released by



238 CODE.

239 Figure 4 shows the daily average differences of DCBs calculated by the model and
240 DCBs of each stations provided by CODE in 2014, and the differences of DCBs
241 calculated by the fixed ionospheric shell height (400 km) and DCBs released by CODE
242 in 2014. The panels for the stations are arranged by their distances to reference station,
243 this is also applied to the following table; from the top panels to the bottom panels, the
244 distance of the corresponding station to the reference station gradually increases. The
245 left and right panels show the daily differences and the histograms of the statistical
246 results in 2014, respectively. For all of the stations, the daily average differences of
247 DCBs calculated by the optimal ionospheric shell height model are reduced compared
248 to the fixed ionospheric shell height. For GOLD and TABV, the reductions are
249 appropriate, the daily average Δ DCBs around 0 have the most days. For the other
250 stations, the reductions are so much that most of the average Δ DCBs are negative. This
251 result shows the improvement of the model seems to be related with the distance to
252 GOLD. Note that some days no result because of missing data. Figure 5 is the same
253 format as Figure 4, which presents the results of Region II. By comparing to the results
254 of fixed ionospheric height, Figure 5 also indicates that the Δ DCB of optimal
255 ionospheric shell heights with PTBB prediction is more concentrated distributed around
256 0 in a statistical sense. Both Figure 4 and Figure 5 present the accuracy of DCB
257 estimation by using optimal ionospheric heights from reference station, namely GOLD
258 and PTBB in this study, can be improved.



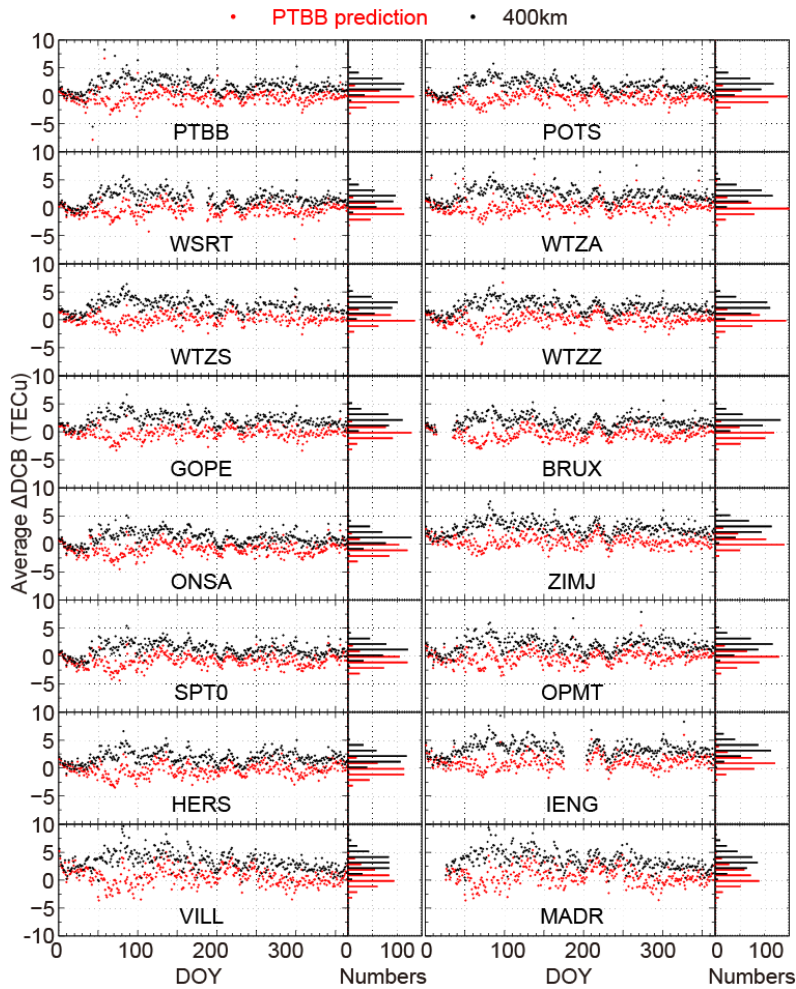
259

260 **Fig.4** Comparisons of the average Δ DCB calculated by the predicted optimal
261 ionospheric shell heights (red dots) and by the fixed ionospheric shell height (black dots)
262 in 2014 for stations in Region I.

263



264



265

266 **Fig.5** Comparisons of the average Δ DCB calculated by the predicted optimal
 267 ionospheric shell heights (red dots) and by the fixed ionospheric shell height (black dots)
 268 in 2014 for stations in Region II.

269

270 Table 2 presents the quantitative statistical results of average Δ DCB in 2014. For



271 all the stations in each region, the mean values and the root mean squares (RMS) by the
 272 optimal ionospheric shell height model are smaller than by the fixed ionospheric height.
 273 For Region I, the improvements of TABV are the most significant. Their mean values
 274 are reduced to 0.12 and 0.08 TECu, respectively; the root mean squares are reduced by
 275 4.43 and 4.33 TECu, respectively. For Region II, the improvement for DCB estimation
 276 are the most obvious for WTZZ, with mean value of Δ DCB decreases from 2.34 to 0.02.
 277 We could note that TABV and WTZZ station are quite close to the reference stations in
 278 each region.

279

280 **Table 2** Statistical results of mean (Δ DCB) in 2014

Station	Average Δ DCB (TECu)		Average Δ DCB (TECu)	
	Optimal Ionospheric Height		Fixed Ionospheric Height	
	Mean	RMS	Mean	RMS
GOLD	0.12	1.82	5.96	6.25
TABV	0.08	2.04	6.06	6.37
QUIN	-1.60	2.31	3.91	4.19
PIE1	-1.38	2.50	4.46	4.84
AMC2	-2.12	2.75	3.09	3.53
PTBB	-0.28	1.23	1.82	2.26
POTS	-0.27	1.00	1.84	2.18
WSRT	-0.41	1.14	1.65	2.10
WTZA	0.09	1.20	2.38	2.73
WTZS	0.14	0.99	2.48	2.76
WTZZ	0.02	1.14	2.34	2.65



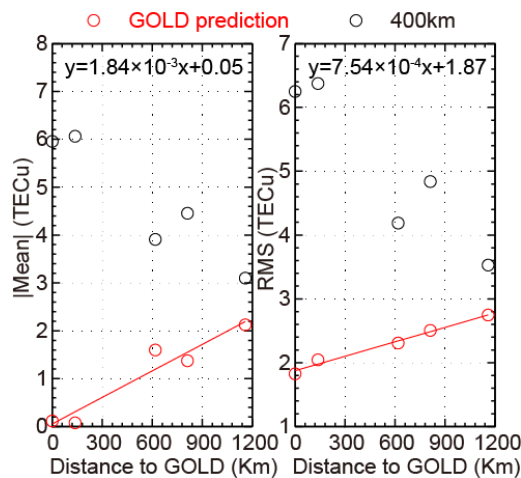
GOPE	-0.17	1.00	2.12	2.41
BRUX	-0.42	1.12	1.86	2.13
ONSA	-0.88	1.40	1.10	1.63
ZIMJ	0.48	1.17	2.87	3.13
SPT0	-0.84	1.40	1.14	1.67
OPMT	-0.29	1.21	1.93	2.35
HERS	-0.37	1.19	1.84	2.19
IENG	1.05	1.57	3.44	3.69
VILL	0.59	1.67	3.30	3.66
MADR	0.66	1.71	3.50	3.86

281

282 Figure 6 and Figure 7 present the relation between the statistical results of average
 283 Δ DCB and the distance to reference stations in each region. The left and the right panels
 284 in each figure show the relation of the absolute mean value and the root mean square
 285 with the distance to GOLD and PTBB, respectively. For all of the stations, the optimal
 286 ionospheric shell height model improves the accuracies of DCB estimation compared
 287 to the fixed ionospheric shell height in a statistical sense; both of the absolute mean
 288 values and the root mean squares become smaller. For the optimal ionospheric shell
 289 height model, the absolute mean values present a positive correlation with the distance
 290 to reference station GOLD and PTBB in each region, as well as the root mean squares.
 291 By using the linear regression, for Region I, the absolute mean value increases at a rate
 292 of about 1.84 TECu per 1000 km and start at about 0.05 TECu. The RMS value
 293 increases at a rate of about 0.75 TECu per 1000 km and starts at about 1.87 TECu.



294 According to the fitting results, the absolute mean value and the RMS less than 1 TECu
295 and 2.25 TECu in the region around GOLD with a radius of 500 km, and less than 2
296 TECu and 2.62 TECu for the region with a radius of 1000 km. For Region II, the
297 absolute mean value increases at a rate of about 0.30 TECu per 1000 km and start at
298 about 0.25 TECu. The RMS value increases at a rate of about 0.41 TECu per 1000 km
299 and starts at about 1.01 TECu. According to the fitting results, the absolute mean value
300 and the RMS less than about 0.40 TECu and 1.21 TECu in the region around PTBB
301 with a radius of 500 km, and less than about 0.55 TECu and 1.42 TECu for the region
302 with a radius of 1000 km. For the two regions, the RMSs presents stronger linear
303 relation with distance comparing to the means.
304

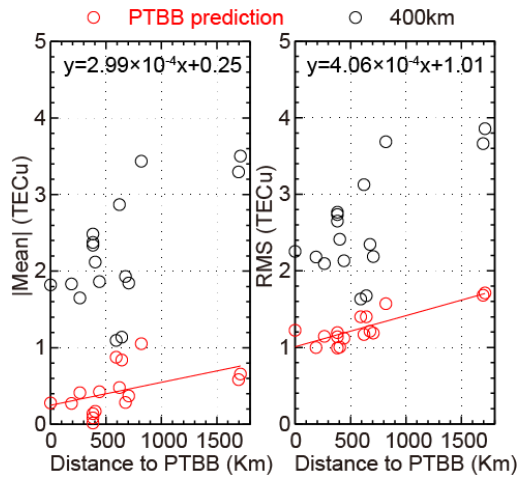


305
306 **Fig.6** Relation of the accuracy for DCB estimation with the distance to GOLD. The red
307 lines are the linear fitting results

308



309



310

311 **Fig.7** Relation of the accuracy for DCB estimation with the distance to PTBB. The red
312 lines are the linear fitting results

313

314

315 **Summary**

316 In this study, we investigate the implementation and validation of optimal ionospheric
317 shell height derived from IGS station to non-IGS station or isolated GNSS receiver. We
318 establish two optimal ionospheric shell height models by the 40th-order of Fourier
319 series based on the data of IGS station GOLD and PTBB in two separate regions. These
320 two models are applied to the stations in each region, where the distance to GOLD
321 ranges from 136.67 to 1159.09 km and the distance to PTBB ranges from 190.82 to
322 1712.27 km. The main findings are summarized as follows:

323 1) The optimal ionospheric shell height model improves the accuracy of DCB



324 estimation comparing to the fixed shell height for all of the stations in a statistical
325 sense. This results indicate the feasibility of applying the optimal ionospheric shell
326 height derived from IGS station to other neighboring stations. The IGS station can
327 calculate and predict the daily optimal ionospheric shell height, and then release
328 this value to the nearby non-IGS stations or isolated GNSS receivers.

329 2) For other station in each region, the error of DCB by the optimal ionospheric shell
330 height increases linearly with the distance to the reference GOLD and PTBB station.
331 For the mean and the RMS of the daily average Δ DCBs, in region I, the slopes are
332 about 1.84 and 0.75 TECu per 1000 km; in region II, the slopes are about 0.30 and
333 0.41 TECu per 1000 km. This results indicate the horizontal spatial correlation of
334 regional ionospheric electron density distribution. For different region, the error at
335 0 km (i.e. the error for the reference station) is different, which should be also
336 considered.

337 As the requirement of this experiment, we just analyze two regions in mid-latitude
338 due to the insufficiency of long-term P1 data. We also ignore the orientation of isolated
339 GPS receivers to the reference station.

340

341 **Acknowledgments**

342 This study is based on data services provided by the IGS (International GNSS Service)
343 and CODE (the Center for Orbit Determination in Europe). This work is supported by



344 the National Natural Science Foundation of China (NSFC grant 41574146 and
345 41774162).

346

347 **Reference**

348 Birch MJ, Hargreaves JK, Bailey GJ (2002) On the use of an effective ionospheric
349 height in electron content measurement by GPS reception. *Radio Sci* 37(1):1015.
350 <https://doi.org/10.1029/2000RS002601>

351 Brunini C, Camilion E, Azpilicueta F (2011) Simulation study of the influence of the
352 ionospheric layer height in the thin layer ionospheric model. *J Geod* 85(9):637–
353 645. <https://doi.org/10.1007/s00190-011-0470-2>

354 Clynch JR, Coco DS, Coker CE (1989) A versatile GPS ionospheric monitor: high
355 latitude measurements of TEC and scintillation. In: *Proceedings of ION GPS-89,*
356 *the 2nd International Technical Meeting of the Satellite Division of The Institute*
357 *of Navigation, Colorado Springs, CO, 22–27 September 1989, pp 445-450*

358 Horvath I, Crozier S (2007) Software developed for obtaining GPS-derived total
359 electron content values. *Radio Sci* 42(2):RS2002

360 Huang Z, Yuan H (2014) Ionospheric single-station TEC short-term forecast using RBF
361 neural network. *Radio Sci* 49(4):283–292

362 Jiang H, Wang Z, An J, Liu J, Wang N, Li H (2018) *GPS Solut.*
363 <https://doi.org/10.1007/s10291-017-0671-0>

364 Klobuchar A (1987) Ionospheric time-delay algorithm for single-frequency GPS users.
365 *IEEE Trans Aerosp Electron Syst* AES-23(3):325–331



- 366 Lanyi GE, Roth T (1988) A comparison of mapped and measured total ionospheric
367 electron content using Global Positioning System and beacon satellite
368 observations. *Radio Sci* 23(4):483–492
- 369 Li M, Yuan Y, Zhang B, Wang N, Li Z, Liu X, Zhang X (2017) Determination of the
370 optimized single-layer ionospheric height for electron content measurements over
371 China. *Journal of Geodesy*. <https://doi.org/10.1007/s00190-017-1054-6>
- 372 Lomb NR (1976) Least-squares frequency analysis of unequally spaced data.
373 *Astrophysics and space science* 39(2):447-462
- 374 Lu W, Ma G, Wang X, Wan Q, Li J (2017) Evaluation of ionospheric height assumption
375 for single station GPS-TEC derivation. *Advances in Space Research* 60(2):286-
376 294
- 377 Mannucci AJ, Wilson BD, Yuan DN, Ho CH, Lindqwister UJ, Runge TF (1998) A
378 global mapping technique for GPS-derived ionospheric total electron content
379 measurements. *Radio Sci* 33(3):565–583
- 380 Nava B, Radicella SM, Leitinger R, Cořson P (2007) Use of total electron content data
381 to analyze ionosphere electron density gradients. *Adv Space Res* 39(8):1292–1297
- 382 Rideout W, Coster A (2006) Automated GPS processing for global total electron
383 content data. *GPS Solut* 10:219–228. <https://doi.org/10.1007/S10291-006-0029-5>
- 384 Sardón E, Rius A, Zarraoa N (1994) Estimation of the transmitter and receiver
385 differential biases and the ionospheric total electron content from global
386 positioning system observations. *Radio Science* 29(3):577–586
- 387 Scargle JD (1982) Studies in astronomical time series analysis. II-Statistical aspects of
388 spectral analysis of unevenly spaced data. *The Astrophysical Journal* 263:835-853



- 389 Schaer S (1999) Mapping and predicting the earth's ionosphere using the global
390 positioning system. Ph.D. dissertation, Astronomical Institute, University of Bern,
391 Bern, Switzerland
- 392 Smith DA, Araujo-Pradere EA, Minter C, Fuller-Rowell T (2008) A comprehensive
393 evaluation of the errors inherent in the use of a two-dimensional shell for modeling
394 the ionosphere. *Radio Sci* 43:RS6008. doi: 10.1029/2007RS003769
- 395 Sovers OJ, Fenselow JL (1987) Observation model and parameter partials for the JPL
396 VLBI parameter estimation software MASTERFIT-1987. NASA STI/Recon
397 Technical Report N, vol 88
- 398 Wang XL, Wan QT, Ma GY, Li JH, Fan JT (2016) The influence of ionospheric thin
399 shell height on TEC retrieval from GPS observation. *Res Astron Astrophys*
400 16(7):016
- 401 Warnant R (1997) Reliability of the TEC computed using GPS measurements—the
402 problem of hardware biases. *Acta Geodaetica et Geophysica Hungarica* 32(3–
403 4):451–459. <https://doi.org/10.1007/BF03325514>
- 404 Wild U (1994) Ionosphere and satellite systems: permanent GPS tracking data for
405 modelling and monitoring. *Geod äisch-geophysikalische Arbeiten in der Schweiz*,
406 Band 48
- 407 Zhao J, Zhou C (2018) On the Optimal Height of Ionospheric Shell for Single-Site TEC
408 Estimation. *GPS Solut.* <https://doi.org/10.1007/s10291-018-0715-0>
- 409 Zus F, Deng Z, Heise S, Wickert J (2017) Ionospheric mapping functions based on
410 electron density fields. *GPS Solut.* <https://doi.org/10.1007/s10291-016-0574-5>
411